UC Berkeley
UC Berkeley Previously Published Works

Title
Neuropercolation: A random cellular automata approach to spatio-temporal neurodynamics

Permalink
https://escholarship.org/uc/item/2qn4778j

Journal
Cellular Automata, Proceedings, 3305

ISSN
0302-9743

Authors
Kozma, R
Puljic, M
Balister, P
<u>et al.</u>

Publication Date
2004

Peer reviewed

Phase Transitions in the Neuropercolation Model of Neural Populations with Mixed Local and Non-Local Interactions

Robert Kozma, Marko Puljic, Paul Balister, and Bela Bollobás

Department of Mathematical Sciences, University of Memphis

Memphis, TN 38152, USA

rkozma@memphis.edu, URL: http://cnd.memphis.edu

and Walter J. Freeman

Division of Neurobiology, University of California at Berkeley

Berkeley, CA 94720, USA

wfreeman@socrates.berkeley.edu, URL:http://sulcus.berkeley.edu

Abstract - We model the dynamical behavior of the neuropil, the densely interconnected neural tissue in the cortex, using neuropercolation approach. Neuropercolation generalizes phase transitions modeled by percolation theory of random graphs, motivated by properties of neurons and neural populations. The generalization includes (i) a noisy component in the percolation rule, (ii) a novel depression function in addition to the usual arousal function, (iii) non-local interactions among nodes arranged on a multi-dimensional lattice. This paper investigates the role of non-local (axonal) connections in generating and modulating phase transitions of collective activity in the neuropil. We derive a relationship between critical values of the noise level and non-locality parameter to control the onset of phase transitions. Finally, we propose a potential interpretation of ontogenetic development of the neuropil maintaining a dynamical state at the edge of criticality.

I. INTRODUCTION

The emergence of collective behaviors in chaotic systems have been studied extensively using various cellular automata and lattice models. The results indicated that low-dimensional structure and collective oscillations may arise on the macroscopic level in a system with extensively chaotic components at the microscopic level (Aihara et al., 19990; Kaneko, 1990; Pomeau, 1993; Marcq et al., 1997). The significance of intermediate-range or mesoscopic effects has been outlined in further studies, with a special emphasis on neurodynamics (Kozma, 1998; Freeman, 1999). Random cellular automata (RCA) appear to have many of the features of these systems, but are simpler to describe, easier to simulate, and are more amenable to rigorous analysis. The present paper concentrates on applying and generalizing the concept of RCA for the description of the dynamics of neural populations.

The theory of random cellular automata is closely related to that of percolation theory, which has been an active area of research in the past decades. Percolation theory lies at the interface of probability theory, combinatorics, and physics (Grimmett, 1999). Interest in various aspects of standard percolation remains high, including estimates of critical probabilities (Bollobás, 1985; Balister, Bollobás, Stacey, 1993). Recently, more and more modifications of the standard percolation models have been studied. In particular, there has been much work on the family of processes know as bootstrap percolation (Aizerman and Lebowitz, 1988; Duarte, 1989; Gravner and McDonald, 1997; Cerf and Cirillo, 1999). Computer experiments have suggested interesting non-trivial large-scale behavior, and many deep mathematical results have been proved about a number of models. Percolation theory deals with large scale properties of certain types of random graphs, often built on d-dimensional lattice Z^d.

In the archetypal percolation problem, the vertices (sites) are the points of a lattice with edges (bonds) joining neighboring sites. In site percolation, sites are open independently with probability p and one wishes to answer questions about the size of the connected components formed by these open sites. In particular, do infinite connected clusters of open sites exist? Similar questions can also be asked about bond percolation, where the bonds are chosen to be open with a certain probability. There are many variants of these problems. For example, in oriented percolation one asks for infinite paths of connected open sites that

travel at each step only in certain directions.

Many percolation problems exhibit phase transitions. In the case of phase transitions, for p less than some critical probability p_{crit} only finite clusters exist, and for $p > p_{crit}$ infinite clusters almost surely exist. Random automata are also closely related to certain models in statistical physics such as the Ising model. This naturally leads to questions about phase transitions and their associated critical exponents which describe properties of systems that are close to a phase transition. Studying phase transitions gains increasing popularity in various research fields beyond physics, including population dynamics, the spread of infectious diseases, social interactions, neural systems, and computer networks (Kauffman, 1993; Crutchfield, 1994; Haken, 1996; Watts, Strogatz, 1998, Newman, 2000).

In the realms of neuropercolation we extend percolation theory to study neural processes (Kozma et al., 2001, 2004). Recent studies explain spatial patterns of phase in beta-gamma EEG activity of human neocortex (Freeman, 2003d-e). Neocortex maintains a stable, scale-free state by homeostatic regulation of neural firing, through which it adapts instantly and globally to rapid environmental changes. The coherent states created by the destabilization of the cortex are called 'wave packets' (Freeman, 2003a-b). Destabilization is initiated at a given, seemingly random point of time and space on the cortex. This resembles phase transition in physical systems, which start at a certain nucleus.

EEG analysis gave spatiotemporal amplitude modulation (AM) patterns of unprecedented clarity (Freeman, 2004a-b) and supported the theory of self-organized criticality in neural dynamics (Bak, Tang, & Wiesenfeld, 1987; Bak, 1996; Jensen, 1998). Spatial gradients of beta-gamma phase revealed multiple co-existing phase patterns that were consistent with a state of self-organized criticality. These results indicate that brains maintain themselves at the edge of global instability by inducing a multitude of small and large adjustments in the form of phase transitions. Phase transitions mean that each adjustment is a sudden and irreversible change in the state of a neural population. Because sensory cortices maintain themselves in highly sensitive meta-stable states, they can transit instantly to any designated part of their state space when destabilized by expected stimuli (Freeman et al., 2004).

Synchronization of neural electical activity while completing cognitive tasks is studied

in various animals, e.g., in cats, rabbits, gerbils, macaque monkeys (Barrie et al, 1996; Ohl, et al, 2001, 2003, Freeman et al, 2003a; Bressler, 2003). It has been demonstrated that using an animal model of category learning, the sorting of stimuli into these categories emerges as a sudden change in the animal's learning strategy. EEG and ECG recordings show that the transition is accompanied by a change in the dynamics of cortical stimulus representation, which represent a mechanism underlying the recognition of the abstract quality (or qualities) that defines the categories. Synchrony of firing of widely distributed neurons in large numbers is necessary for emergence of spatial structure in cortical activity by reorganization of unpatterned background activity.

Oscillations measured by EEG, MEG, and other brain monitoring techniques arise from extensive feedback interactions among neurons densely connected in local neighborhoods, in combination with the effects of long axons. Axonal effects have high conduction velocities and support synchronization over large areas of cortex (Bressler and Kelso, 2001, Bressler, 2002; Freeman, 2004a-b), creating small-world effects (Watts and Strogatz, 1998; Wang and Chen, 2003) in analogy to the rapid dissemination of information through social contacts. Small-world networks have certain preferential attachment rules between vertices that make the network diameter much smaller than regular ones, like grids and lattices. The importance of long-distance correlations has been emphasized by numerous brain theorists (e.g., Ingber, 1995; Hoppenstaedt and Izhkevich, 1998; Haken, 1999; Friston, 2000; Linkenkaer-Hansen et al., 2001; Kaneko and Tsuda, 2001; Kozma et al., 2003; Stam et al., 2003). In certain networks, like the www, biological systems, the degree distribution follows a power law, i.e., it is scale-free. Crucial developments have been reported concerning scale-free networks (Albert & Barabási, 2002; Barabási & Bonabeau, 2003; Bollobás & Riordan, 2003).

Neuropercolation approach has some common aspects with the small-world and scale-free network studies. However, key differences have to be pointed out. While scale-free network studies strongly rely on established methods of statistical physics, neuropercolation goes beyond existing tools. The neural tissues in the brains, called neuropil, have unique properties requiring not just new models, but completely new mathematical methods of thorough analysis. Neuropercolation is a generalization of cellular automata, Hopfield memory arrays and Conway's game of life (Hopfield, 1982; Berlekamp et al., 1982), by merging the concepts of random graph theory (Erdos & Renyi, 1960; Bollobás, 1985) and non-local interactions

represented by axonal connections. It bridges the gap between Ising-type models and mean-field approaches (Kozma et al, 2002; Balister, Bollobás, Kozma, 2003). Our studies identify several key factors that determine phase transitions in our neural models, including endogenously generated noise and the structure and extent of the non-locality of neural populations. The resulting novel tools have been used to study the intricate complexity of various dynamic behaviors of neural populations (Puljic & Kozma, 2003).

The present paper starts with the description of basic principles and formalism of neuropercolation. We introduce results of mean field models as well as locally connected RCA lattices. Next the critical behavior in mixed local and non-local models is described. We build phase diagrams to characterize the relationship between critical noise and extent of non-locality. This is followed by the characterization of a potential developmental process in brain after birth and early childhood, which may be responsible for maintaining dynamical state of brains at the edge of criticality.

II. OVERVIEW OF PHENOMENOLOGY OF NEUROPERCOLATION

A. Role of Dynamics in Neural Populations

We model the dynamical behavior of the neuropil, the densely interconnected neural tissue in the cortex. Most synaptic activity in the brain occurs in the neuropil. Neuropil is a unique felty substance, believed to be one of the most highly organized in the Universe. It represents a complicated spatial network comprising interconnected neuronal processes intermingled with irregularly shaped processes of astrocytic glia (Peters et al., 1991). Neural populations stem ontogenetically in embryos from aggregates of neurons that grow axons and dendrites and form synaptic connections of steadily increasing density. At some threshold the density allows neurons to transmit more pulses than they receive, so that an aggregate undergoes a state transition from a zero point attractor to a non-zero point attractor, thereby becoming a population. Interacting excitatory and inhibitory populations produce periodic, limit cycle oscillations. At the next level of complexity, an increasing volume of research aims at the interpretation of dynamic brain activity in terms of aperiodic, chaotic processes (Skarda & Freeman, 1987; Schiff et al, 1994; Arhem et al., 2000; Dafilis et al., 2001; Korn

& Faure, 2003).

A chaotic system has the capacity to create novel and unexpected patterns of activity. It can jump instantly from one mode of behavior to another. It retains in its pathway across its basins a history, which fades into its past, just as its predictability into its future decreases. Phase transitions between chaotic states constitute the dynamics that explains how brains perform such remarkable feats as abstraction of the essentials of figures from complex, unknown and unpredictable backgrounds, generalization over examples of recurring objects, reliable assignment to classes that lead to appropriate actions, planning future actions based on past experience, and constant updating by way of the learning process (Freeman, 1999). Below, we describe certain topological and dynamical properties of the neuropil, ro support modeling phase transitions in brains.

B. Random Cellular Automata Formalism

General models of random cellular automata (RCA) are well-documented, see (Toom et al.; Gacs, 1990; Maes and Velde, 1997; and others). Here we limit our discussions to a model on the 2-dimensional discrete torus Z_n^2. Let $x = \{i, j\}$ is a site in Z_n^2. The activation of site x at time t $a_x(t)$ can be 0 or 1 The fate of each site will be influenced by the sites in the neighborhood $\Lambda(x)$. Introduce $s(x)$ as the arousal function and $r(x)$ as the depression function. The arousal function gives the probability that an inactive site becomes active, while the depression function is the probability that an active site becomes inactive at the next step. At time 0, the sites are active with probability p. At each time step t, every site is updated simultaneously according to the rules:

$$s(x) = \{\varepsilon_1, \quad if \quad C_t; \quad 1 - \varepsilon_1 \quad if \quad \neg C_t\}, \tag{1}$$

$$r(x) = \{\varepsilon_2, \quad if \quad C_t ; \quad 1 - \varepsilon_2 \quad if \quad \neg C_t\}. \tag{2}$$

Here we introduced event C_t as follows:

$$C_t : \sum_{k \in \Lambda(x)} a_k(t) \leq \frac{|\Lambda(x)|}{2} \tag{3}$$

C_t means that the majority of sites in the neighborhood $\Lambda(x)$ are inactive at time t. Here $|\Lambda(i,j)|$ denotes the cardinality of neighborhood $\Lambda(i,j)$. For example, in a 2-dimensional lattice with local interactions, we have $|\Lambda(i,j)| = 5$, when self-connection is included.

In the case when no cell can change from active to inactive ($r(x) = 0$ for all x) we recover the bootstrap percolation model. Clearly, the family of random cellular automata is much richer than the family of bootstrap percolations. In particular, if all the probabilities are 0 or 1 we recover the theory of deterministic cellular automata, such as that of Conway's Game of Life (Berlekamp et al., 1982). These models are known to be capable of producing extremely complex behavior. On the other hand, if we choose $j(x)$, $r(x) \neq 0$, 1 for all x, then there is no need for an initial probability p, and with a suitable choice of the arousal and depression functions, we may achieve that the system hovers around a certain density of active sites.

C.   Mean Field Random Cellular Automata Models

Phase transitions in mean field random cellular automata models are analyzed in details by (Balister et al., 2003). Here we summarize the results for the case of a finite grid or torus over Z^2. In the mean field model instead of taking $|\Lambda|$ specified neighbors, we take $|\Lambda|$ elements of the grid at random with replacement. It is clear that the mean field model does not depend on the topology of the grid, and the only information of relevance is the cardinality

$$X_t = \sum_{k \in Z_n^2} a_k(t). \tag{4}$$

We define ρ_t to be X_t/N where $N = n \times n$ is the size of the finite grid or torus. Thus $\rho_t \in [0,1]$ gives the density of active points.

Let us consider the symmetric model $s = 1 - r$. It is readily shown that the mean field model in this case has one fixed point at $\rho = 0.5$ for $\varepsilon \in [\varepsilon_c, 0.5]$, but for $\varepsilon < \varepsilon_c$ the fixed point $\rho = 0.5$ is unstable and there are two other fixed points which are stable (Balister et al., 2004). Here we illustrate the results in the 2-dimensional lattice, where the critical
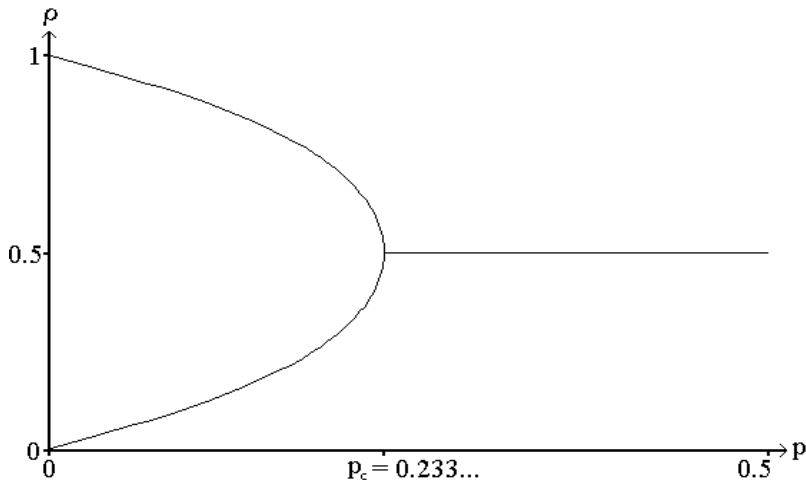
FIG. 1: Activation density ρ of the mean field model with $p_c = 0.233$.

probability $\varepsilon_c = \frac{7}{30}$. Indeed, let us write the condition for the fixed point density as:

$$d = (1 - \varepsilon)\left(\sum_{i=0}^{\lfloor |\Lambda|/2 \rfloor} B(|\Lambda|, i)d^{|\Lambda|-i}(1-d)^i \right) + \varepsilon\left(1 - \sum_{i=0}^{\lfloor |\Lambda|/2 \rfloor} B(|\Lambda|, i)d^{|\Lambda|-i}(1-d)^i\right), \quad (5)$$

where $B(a, b)$ is the binomial coefficient. Considering $|\Lambda| = 5$, one readily obtains the condition for stable solution as $\varepsilon_c = 0.5 - (12d^4 - 24d^3 + 8d^2 + 4d + 2)^{-1}$. After substituting the value $d = 0.5$ at criticality, we get $\varepsilon_c = \frac{7}{30}$. The above equation describing the fixed points approximates power law relationship with very good accuracy:

$$|d - 0.5| \propto (\varepsilon_c - \varepsilon)^\beta, \quad (6)$$

where $\beta \approx 0.5$. Figure 1 illustrates the stable density values for $0 \leq \varepsilon \leq \varepsilon_c$ as described by the above equation.

D. Local Majority Percolation Models

Theoretical description of phase transitions in local RCA is a very difficult problem. Mathematical description of phase transitions in a narrow class of RCA with $\varepsilon \approx 0$ are given in (Balister et al., 2004). Namely, we gave a rigorous proof of the fact that the model spends

a long time in either low- or high-density configurations before crossing very rapidly to the other state. Fairly good bounds have been proven on the very long time the model spends in the two essentially stable states and on the very short time it takes to cross from one essentially stable state to another. This result, in fact, gives a theoretical justification of the terminology 'neuropercolation' of our approach. It is expected that these results can be generalized to a wider range of ε. However, conditions near the critical regime of RCAs are not tractable by rigorous mathematical methods at present.

In the following discussions, we use extensive numerical simulations to study the critical behavior of the neuropercolation model. The simulation was run on a 2-dimensional torus Z_n^2 of size up to 256x256. The next state of the site at a given location will be given by the majority of the states of itself and its four nearest neighbors. All the sites will be updated simultaneously at a certain time t. At any time instant the average activation $\rho(t)$ has been calculated as the mean value over all lattice points, which is analogous to the magnetization parameter of Ising models (Makowiec, 1999).

As we vary ε in the range $[0, 0.5]$, the model exhibits a behavior similar to that seen in the mean field model. For small ε there are two stable states, one with low density ρ and one with high density $1 - \rho$. There is a probability that the system switches between high and low density states. This probability can be made very small by increasing the grid size n. For ε close to the critical probability, one sees large grid regions with high density and large regions with low density evolving in time and space. The variance of the density drastically increases as $\varepsilon \to \varepsilon_c$. An important difference between mean field models and local RCA is that the critical probability is significantly lower in RCA with $\varepsilon_c \approx 0.1342$. For $\varepsilon_c < \varepsilon < 0.5$ the stationary density distribution of ρ_t is unimodal for a sufficiently large but finite lattice. For $\varepsilon < \varepsilon_c$ the distribution becomes bimodal, as one would expect from the mean field model.

In the characterization of RCA, we follow the methodology applied by (Makowiec, 1999), based on Binder's finite-size scaling theory (Binder, 1981). Details of this methodology will be given in the next section, where models with nonlocal connections are described. Here we summarize the results obtained for the local RCA with majority voting rule. According to finite-size scaling theory, the following power laws are expected to hold:

TABLE I: Comparison of RCA and Other Lattice Models

	β	γ	ν	I_{error}
RCA[1]	0.1308	1.8055	1.0429	0.02
TCA[2]	0.12	1.59	0.85	0.13
Ising(2D)[3]	0.125	1.75	1	-
CML [4]	0.115	1.55	0.89	0.00

(1) Kozma et al. (2003), (2) Makowiec (1999); (3) Cipra (1987);

(4) Marcq et al. (1997)

$$\rho \sim (\varepsilon - \varepsilon_c)^\beta \; for \; \varepsilon_c \; \leq \varepsilon \tag{7}$$

$$\chi \sim |\varepsilon - \varepsilon_c|^{-\gamma} \; for \; \varepsilon \; \rightarrow \varepsilon_c \tag{8}$$

$$\xi \sim |\varepsilon - \varepsilon_c|^{-\nu} \; for \; \varepsilon \; \rightarrow \varepsilon_c \tag{9}$$

In the above equations, the following quantities are used: critical probability ε_c, susceptibility χ, and correlation length ξ. The estimated values of the critical exponents β, γ, ν are given in Table I. The results are reproduced from (Kozma et al., 2003), and they are compared with exponents obtained by the 2-dimensional Ising model, Toom Cellular Automata (TCA) based on (Makowiec, 1999), and coupled map lattice model (CML) using (Marcq et al., 1997). For the Ising model, the following identity function holds:

$$2\beta + \gamma = 2\nu \tag{10}$$

Table I contains the error of the identity function, which is defined as the difference of the left hand side and right hand side of the above equation $I_{error} = 2\beta + \gamma - 2\nu$. It has been concluded that the RCA with local majority voting satisfies the exponential scaling relationships very well and it belongs to the Ising, or possibly to a weak-Ising universality class (Kozma et al., 2003).

III.   CRITICAL BEHAVIOR IN MIXED MODELS

A.   Definition of Mixed Models

In the previous discussions we have introduced simplified models with either mean-field interactions, or RCAs with local neighborhoods in the d-dimensional lattice. In this section we turn our attention to more realistic models of the neuropil with a mixture of local and non-local connections. In our model, local connections correspond to dendritic interactions in the arbor of the neuron, while non-local connections describe far-reaching effects through long axons. In our treatment we want to preserve as much as possible from the results obtained previously, in particular, concerning phase transitions. At the same time, we generalize the previous results, to describe better the dynamics of cortical processes.

The mixed model has neurons with local and non-local connections in the 2-dimensional lattice; see Figs. 2 and 3. Starting with a lattice having only local neighborhoods, we add non-local (remote) connections to randomly selected sites. The cardinality of the neighborhood does not change. Accordingly, for each non-local neighbor we cut a randomly selected local neighbor. The locations of remote connections are fixed and chosen randomly at the initiation. In the updates, we use the majority rule as previously. The local neighborhood of site $x = \{i, j\}$ is given as $\Lambda(\{i,j\}) = \{\{i-1,j\}, \{i+1,j\}, \{i,j\}, \{i,j-1\}, \{i,j+1\}\}$. An example of the neighborhood in case of an additional remote neighbor is: $\Lambda(\{i,j\}) = \{\{i,j\}, \{i,j-1\}, \{i,j+1\}, \{i+1,j\}, \{i+1,j+1\}\}$; see Fig. 2.
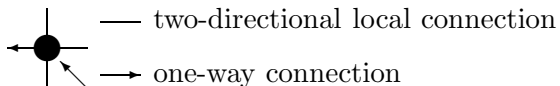

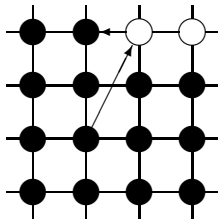FIG. 2: Example of inactive site with local and remote connections.

FIG. 3: Example of a lattice with local and remote connections.

B.   Experiments with Mixed Models

Examples of temporal dynamics of a system with 5% of the sites having one remote neighbor are shown in Fig. 4. Results are obtained with experiments on 128x128 lattices for 10^6 steps. The figures illustrate subcritical ($\varepsilon = 0.146$), critical ($\varepsilon = 0.147$), and supercritical ($\varepsilon = 0.147$) configurations, respectively.

Starting with a lattice with randomly initiated site activation and having a small value of ε, the activity of the network quickly stabilizes in either mostly active or mostly inactive mode of behavior. Because the systems are of finite size, they jump after a sufficiently long time from one mode of behavior to the other. Figure 4 shows that the two modes are symmetrical. As ε_c increases, jumps between the two stable states become more frequent. Beyond the critical probability ε_c the oscillations becomes unimodal and the oscillation intensity decreases.

Figure 5 shows the average densities as the functions of ε for four typical systems: the systems with no remote neighbors (local), the systems with 25% sites having one remote connection (25% (1)), the systems with 100% sites having one remote connection (100% (1)), and the systems with 100% sites having four remote connections (100% (4)).

Figure 6 shows the typical spatial patterns for various configurations of remote neighbors. We applied 3 levels of ε in each configuration. The applied ε values correspond to subtrical, critical, and supercritical regimes. Let us define the parameter $m(t) = \rho(t) - 0.5$, which can be interpreted as magnetization in our model. The sites have been initiated sites as mostly active. On the left side in Fig. 6, ε is far below ε_c. In the middle part, $\varepsilon \approx \varepsilon_c$. On the right side of Fig. 6, ε is greater then ε_c. We can observe that subcritical and
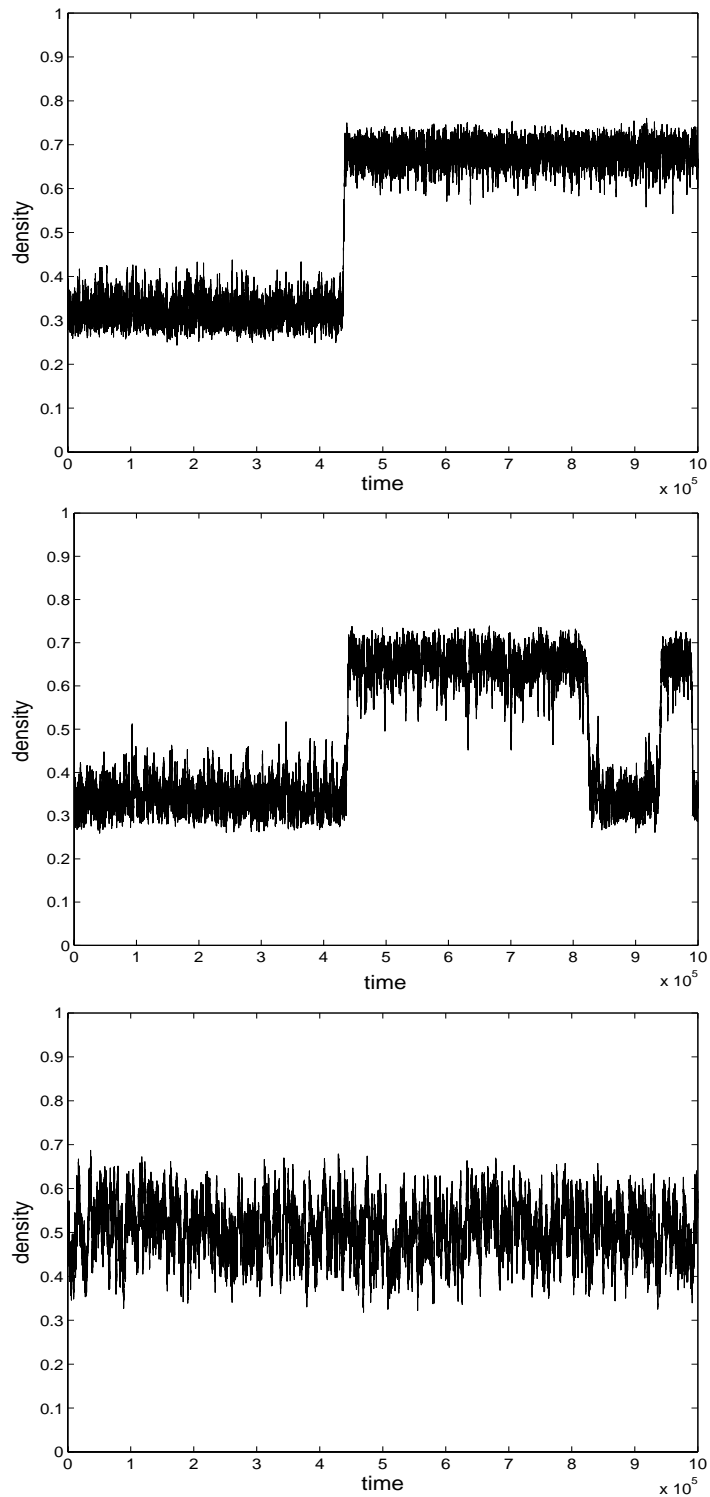
FIG. 4: Typical temporal behavior of the active sites for 10^6 steps. 5% of the sites have one randomly selected remote neighbor. Lattice size is 128x128; (a) $\varepsilon = 0.146$, (b) $\varepsilon = 0.147$, (c) $\varepsilon = 0.151$.
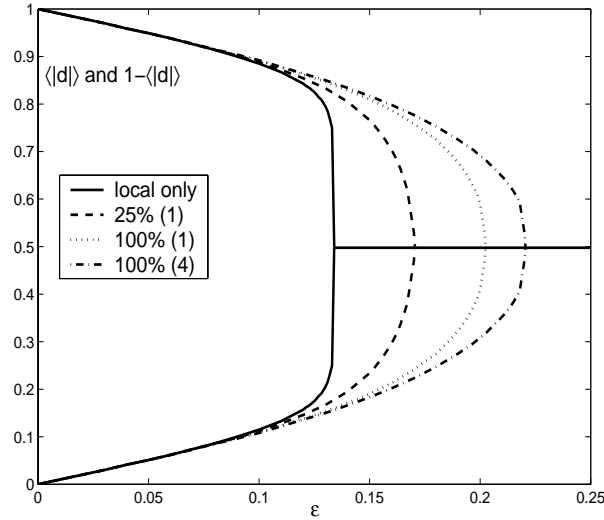
FIG. 5: Activation density as the function of ϵ for the systems with no remote neighbors, 25%(1), 100%(1), and 100%(4).

supercritical regimes give spatial distributions indicating ferromagnetic and paramagnetic states, respectively, as described by Ising models. In the case of critical noise level (middle column), a spatial clustering is apparent, especially for configurations with smaller number of remote connections, i.e., on Fig. 6 (a) and (b).

C. Critical Exponents of Mixed Models

The probability distribution of the density (magnetization) is bimodal for $\varepsilon < \varepsilon_c$. S ε increases, the peaks of the probability distribution function get closer to each other and its peakedness increases. Measures of the peakedness are given by the kurtosis, the 4th moment of the probability distribution. Peakedness is given by:

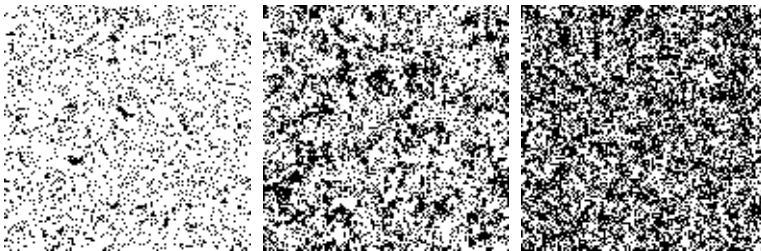$$\alpha_4(\rho) = \frac{\langle (\rho - 0.5)^4 \rangle}{\langle (\rho - 0.5)^2 \rangle^2} \tag{11}$$

Binder defines the 4th order cumulants of the magnetization as follows:

$$U(l, \epsilon) = 1 - \frac{\langle m^4 \rangle}{3 \langle m^2 \rangle^2} \tag{12}$$

Finite-size scaling theory implies that the interpolated values of Eq. (12) are expected to intersect at a unique point at the critical state, independently of the lattice size, which
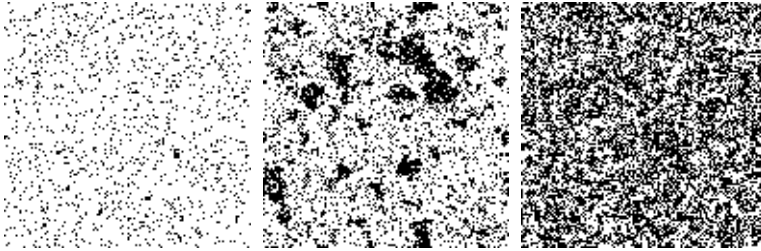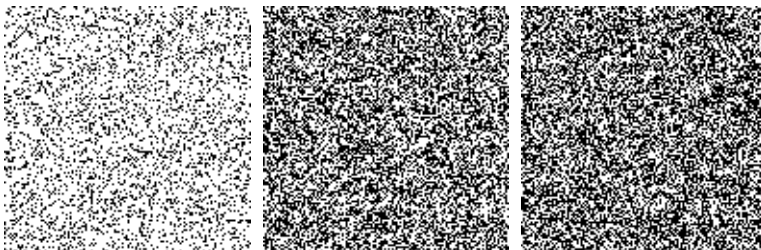
(a) Local model; $\varepsilon = 0.08, \varepsilon = 0.134, and \varepsilon = 0.25$

(b) Mixed model: 25%(1) with $\varepsilon = 0.12, \varepsilon = 0.170, \varepsilon = 0.25$

(c) Mixed model: 100%(1) with $\varepsilon = 0.14, \varepsilon = 0.204, \varepsilon = 0.25$

(d) Mixed model: 100%(4) with $\varepsilon = 0.16, \varepsilon = 0.224, \varepsilon = 0.25$

FIG. 6: The systems from top to bottom; (a) no remote neighbors; (b) 25% of sites have one remote neighbor 25%(1); all sites have one remote neighbor 100%(1); and all 4 neighbors are remote 100%(4).

we denote here as l. The location of this intersection will give ϵ_c. Following (Makowiec, 1999), we write the scaling equations near the critical point, to obtain scaling exponents ν,

β, and γ. Exponent ν describes scaling of the correlation length, and it is obtained from the obtained 4th order cumulant $U(l, \varepsilon)$ as follows:

$$\frac{dU(l, \varepsilon_c)}{d\varepsilon} \propto l^{\frac{1}{\nu}} \tag{13}$$

For the magnetization, the following relationship holds:

$$\langle |d(l, \varepsilon_c)| \rangle \propto l^{-\beta/\nu} \tag{14}$$

where the average magitute of the magnetization is given by:

$$\langle |d| \rangle = \frac{1}{n} \sum_{t=1}^{n} |d(t) - \frac{1}{2}|. \tag{15}$$

Susceptibility χ is defined as follows:

$$\langle \chi(l, \varepsilon_c) \rangle = l^2 (\langle |d(l, \varepsilon_c)|^2 \rangle - \langle |d(l, \varepsilon_c)| \rangle^2) \tag{16}$$

Susceptibility χ satisfies the scaling relationship:

$$\langle \chi(l, \varepsilon_c) \rangle \propto l^{\gamma/\nu - 2} \tag{17}$$

D. Estimating Critical Parameters in Mixed Models

Experiments have been conducted for four different lattice sizes $l = 64, 80, 96$, and 112, respectively. For each lattice size, we have performed experiments with the following lattice configurations: system with no remote connections, and systems with remote connections 25%(1), 100%(1), and 100%(4), i.e, 25% and 100% of sites having 1 remote neighbor, and 100% of sites having 4 remote neighbor, respectively. The case of model with local connections only have introduced in the previous section. Results with mixed configurations are shown in Fig. 7. Simulations have been conducted with at least $5 * 10^7$ steps or until

TABLE II: Critical Exponents in Mixed Models

|	ε_c	β	γ	ν	I_{error}
local	0.1342	0.1308	1.8055	1.0429	0.02
25%(1)	0.1702	0.3071	1.1920	0.9504	0.09
100%(1)	0.2032	0.4217	0.9873	0.9246	0.02
100%(4)	0.2227	0.4434	0.9371	0.9026	0.02

$\langle|0.5 - d|\rangle \leq 0.00005$. Using linear interpolations of the scaling relations in the previous section, we determine the critical exponents for all the systems and configurations. The obtained critical parameters are summarized in Table II.

The first step is to calculate ε_c; see Fig. 7 (a), top row. Having ε_c, ν equals to a slope of linearly interpolated $dU(64, \varepsilon_c)/d\varepsilon$, $dU(80, \varepsilon_c)/d\varepsilon$, $dU(96, \varepsilon_c)/d\varepsilon$, and $dU(112, \varepsilon_c)/d\varepsilon$ in $log(dU)$ vs. $log(l)$ coordinates. ν is obtained in similar way, using $d(log|d(\varepsilon_c)|)/d\varepsilon$, $d(log|d(\varepsilon_c)|^2)/d\varepsilon$, and $d(log|d(\varepsilon_c)|^4)/d\varepsilon$; see Fig. 7 (b), second row from the top. $-\beta/\nu$ equals to the slope of linearly interpolated $\langle|d(64, \varepsilon_c)|\rangle$, $\langle|d(80, \varepsilon_c)|\rangle$, $\langle|d(96, \varepsilon_c)|\rangle$, and $\langle|d(112, \varepsilon_c)|\rangle$ in $log(\langle|d|\rangle)$ vs. $log(l)$ scale. β can also be calculated using $|d(\varepsilon_c)|^2$, or using $|d(\varepsilon_c)|^4$; see Fig. 7 (c), third row from the top. To get the ratio $-2\beta/\nu$ and $-4\beta/\nu$, $\langle|d|^2\rangle$ and $\langle|d|^4\rangle$ are used similarly as the $\langle|d|\rangle$ for the ratio β/ν. γ equals to the slope of linearly interpolated $\langle\chi(64, \varepsilon_c)\rangle$, $\langle\chi(80, \varepsilon_c)\rangle$, $\langle\chi(96, \varepsilon_c)\rangle$, and $\langle\chi(112, \varepsilon_c)\rangle$ in $log(\langle\chi\rangle)$ vs. $log(l)$ scale; see Fig. 7 (d), bottom row.

Identity function $2\beta + \gamma = 2\nu$ holds for Ising systems. The error of this identity I_{error} is used to verify the conducted critical exponents estimation; see Table II. We conclude that the critical exponents significantly deviate from each other and, in particular, from the Ising model. Parameters ν and γ are decreasing, while β and ε_c are increasing, as the number of remote connections increases. ε_c is lower for more structured systems. Still, the identity function is satisfied in most cases with reasonable accuracy. It is expected that the somewhat larger errors can be further reduced if the number of iterations is increased.
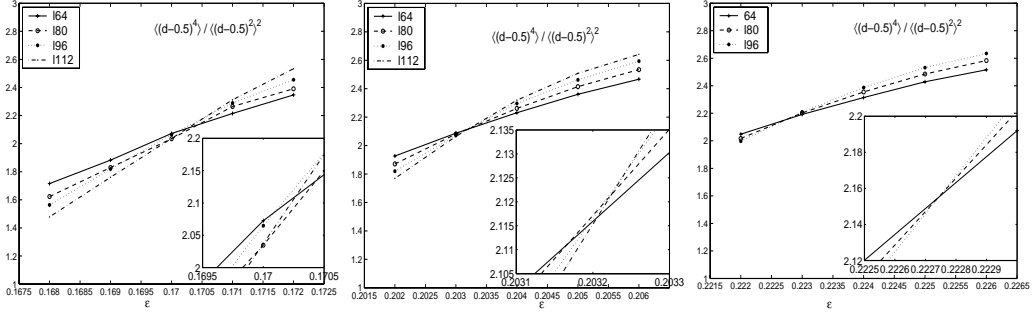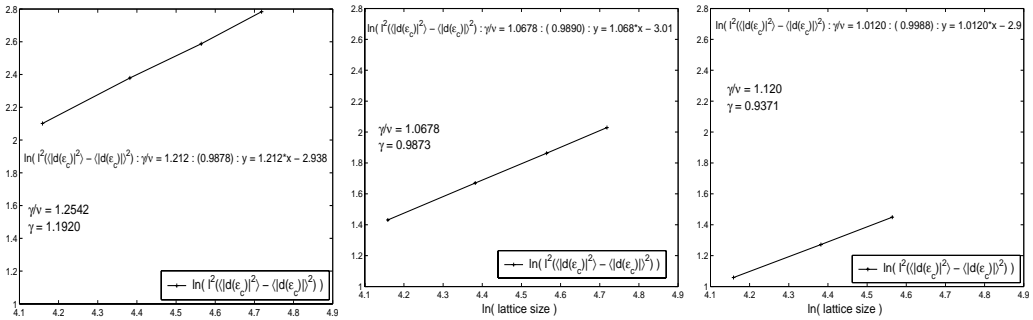
Estimation of the critical probability ε_c.
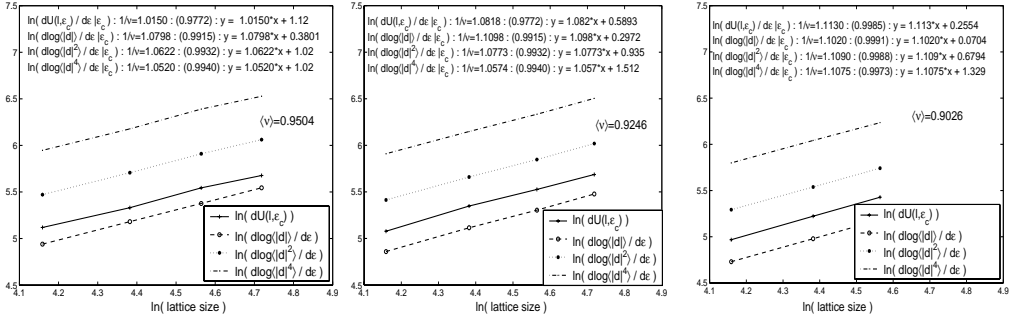
Estimation of the critical exponent of the correlation length ν.
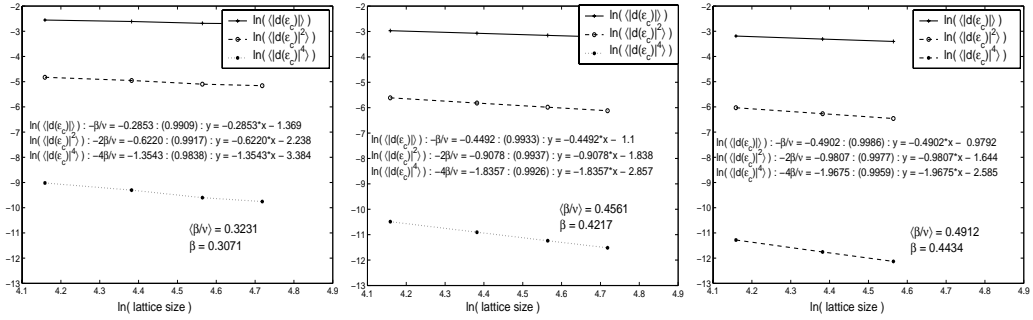
Estimation of the critical exponent of magnetization β.

Estimation of the critical exponent of susceptibility γ.

FIG. 7: Estimation of various critical parameters of mixed models using Binder's method of finite-size scaling. Experiments have been conducted with $l \times l$ lattices of size $l = 64$, 80, 96, and 112.
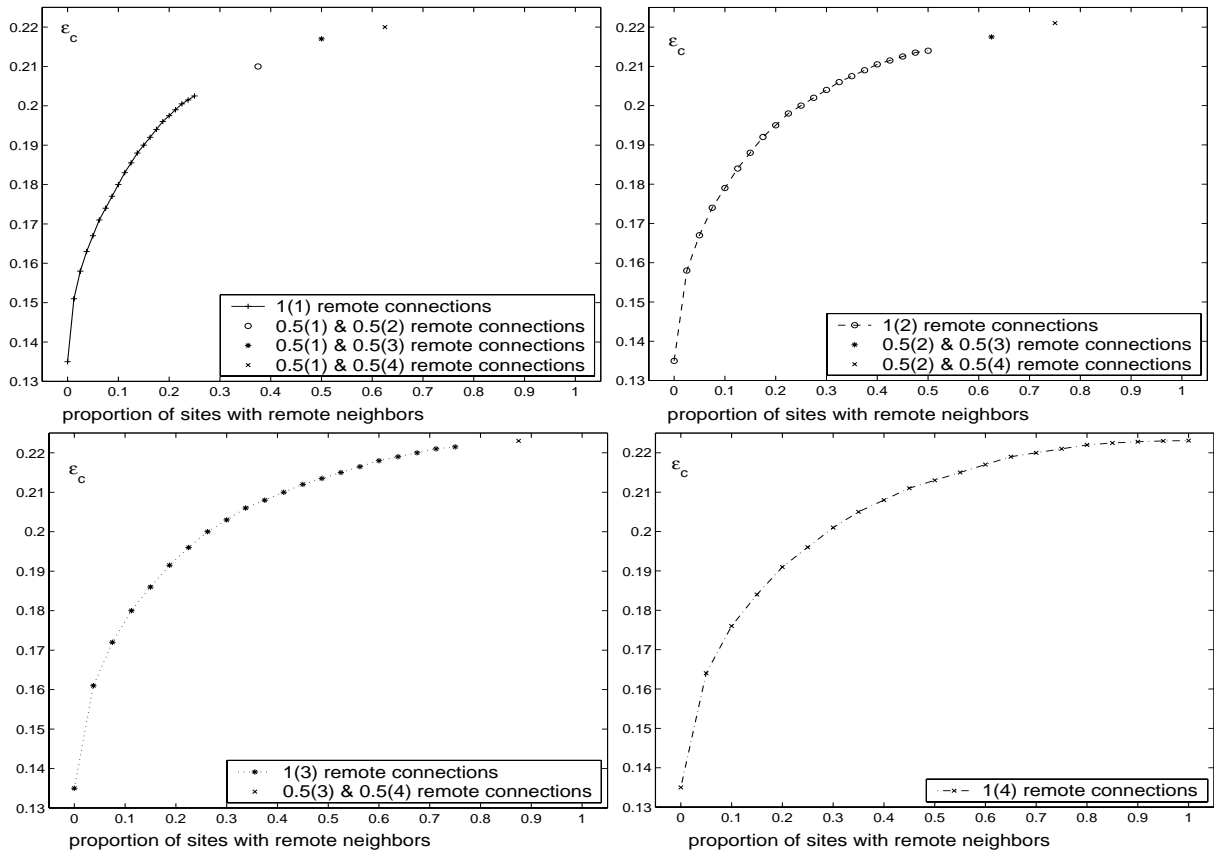
FIG. 8: ε_c as the function of the proportion of remote connections; (a)combinations of 50% of each 1 and 1, 1 and 2, 1 and 3, and 1 and 4 remote connections; (b) 50% of each 1 and 1, 2 and 3, and 2 and 4 remote connections; (c) 50% sites having 3 and 4 remote connections; (d) all sites have 4 remote connections.

IV.   DENSITY OF NON-LOCAL LINKS AS CRITICAL PARAMETER

In this section we study the quantitative relationship between the density of non-local connections and critical probability ε_c. Previously we have observed that ε_c increases as the density of remote connections increases. We have conducted a large number of experiments with various system configurations to quantify this relationship. In Fig. 8 a-d, ε_c is shown as a function of the proportion of sites with remote connections for many different systems. To calculate ε_c, we applied the same method as before. In the experiments in Fig. 8 we used shorter runs that previously, as less accuracy is sufficient if we do not aim at determining the critical exponents.

For a given number of remote links, usually there is a range of critical probabilities, depending on the actual way the connections are distributed. If the remote neighbors are evenly distributed among the neurons in the network, we get higher ε_c values. At the same time the ε_c values are lower when the remote neighbors are clustered towards a fewer number of sites. It is concluded that the density of nonlocal connections acts as a critical parameter. Accordingly, by varying nonlocal connectivity while all other parameters of the system are fixed, we can produce critical behavior and phase transitions. This allows us to build phase diagrams in the state space of noise and nonlocality of interactions.

Such a phase diagram is shown in Fig. 9 where results obtained by various configurations are combined. Network structures with higher number of reciprocal remote connections make the system more vulnerable to disturbances, when the system evolution is governed by the random majority rule. One-way connections increase the network resistance to noise-induced phase transitions. This is due to the fact that a neighborhood is more likely to sustain a continued activation state with mutual reinforcement of two-way local connections following the majority rule. In the case of only local or only remote neighbors, obviously we can have only one configuration giving ε_c values of 0.13428 and 0.2242, respectively.
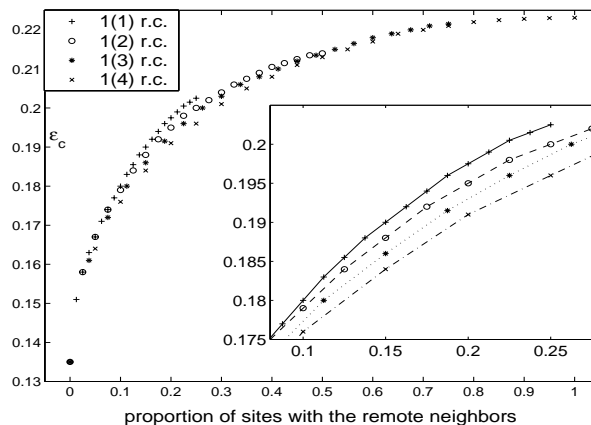

FIG. 9: Integrated view of the relationship between critical noise and the proportion of remote connections for all studied network configurations.

V.   EVOLUTION OF CRITICAL BEHAVIOR IN THE NEUROPIL

We propose the following hypothesis on the emergence of critical behavior with the potential of frequent phase transitions in the neuropil. The neural connectivity is sparse in the neuropil at the embryonic stage. Following birth, the connectivity increases and ultimately reaches a critical level, at which the neural activity becomes self-sustaining. The brain as a collective system is at the edge of criticality, and it now can undergo repeated phase transitions in a self-organized way, under the influence of external and internal factors. We suggest to implement this approach in a computational model as follows:

- Start with an initial population of nonlinear units, which model neural populations with given local properties;

- Incrementally increase the long-range connectivity using any desired strategy, producing, e.g., a scale-free network with preferential attachment, or other objects;

- Stop changing the connectivity when the critical state is approached. From this stage on, the structure is essentially fixed. Modifications still happens; e.g., due to learning effects;

- Use the effects of inputs and endogeneous noise to balance the system at the edge of phase transitions during its operation;

- Operate the system through repeated phase transitions as it processes, retrieves, and transforms data.

The above strategy is schematically illustrated in Fig. 10. By way of structural evolution, the neuropil evolves toward regions of criticality or edge-of-criticality. Once the critical regions are established, the connectivity structure remains essentially unchanged. However, by adjusting the noise and/or gain levels, the system can be steered towards or away from critical regions. This is a control mechanism that provides the conditions to phase transitions in the neuropil. Obviously, the outlined mechanism is incomplete and in realistic neural systems a host of additional factors play crucial role. However, the given mechanism is very robust and it may provide the required dynamical behavior in a wide range of real life conditions.
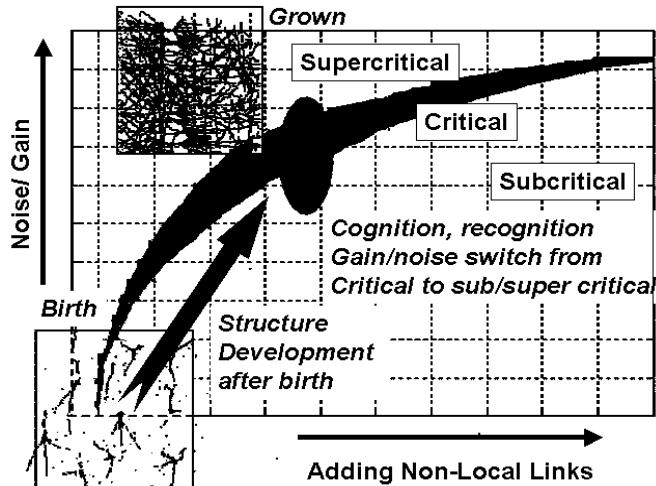
FIG. 10: Illustration of self-organization of critical behavior in the percolation model of the neuropil

VI.   CONCLUSIONS

By describing certain topological and dynamical properties of the neuropil, we aim at modeling phase transitions in brains. Destabilization by sensory stimuli and sudden changes in the spatio-temporal neurodynamics in the cortex resembles phase transitions in phyiscal systems. Phase transitions are much more complex in brains than in physics. In brains, transitions to a more organized phase are intermittent. The transition to the highly organized state happens in a matter of 3-5ms. Multiple states commonly exist in both time and space in each cerebral hemisphere.

We suggested a novel method for modeling and functioning of the neuropil. The neuropercolation approach to phase transitions in the neuropil has the prospect of creating powerful, robust computational models that match the performance of neural systems. Our study identifies key control parameters of this process, i.e., communication noise, relative proportion of axonal connections. Phase diagram has been constructed and has been used to outline a hypothesis of self-organized development of the neuropil.

The proposed method of controling phase transitions in the neuropil will be tested both in discrete neuropercolation models and in the continuous domain of K models, which is based on ordinary differencial equations (Kozma & Freeman, 2001). We explore the dynamics of spatio-temporal patterns in the neuropercolation model. In particular we will study

conditions that may lead to the emergence of phase cones and itinerant chaotic dynamics, as observed by brain monitoring methods.

VII.   ACKNOWLEDGMENTS

---

[1] Aihara, K., Takabe T., Toyoda M., (1990). Chaotic neural networks, Phys. Lett. A, 144 (6-7), 333-340.

[2] Aizeman and Lebowitz, *Metastability effects in bootstrap percolation*, J. Phys. A **21** (1988) 3801–3813.

[3] Albert, R., Barabási, A.L., "Statistical mechanics of complex networks," Reviews of Modern Physics 74, 47 (2002).

[4] Arhem, P., C. Blomberg, H. Liljenstrom, Disorder versus order in brain function, Progr. Neural Processing, Vol. 12, ISBN 981-02-4008-2, World Scientific, 2000.

[5] Bak, P., "How Nature Works - The Science of Self-Organized Criticality," Springer Verlag, N.Y., 1996.

[6] Bak, P., Tang, C., Wiesenfeld, K., Phys. Rev. Lett., 59, 381, 1987.

[7] P.N. Balister, B. Bollobás, and A.M. Stacey, *Upper bounds for the critical probability of oriented percolation in two dimensions.* Proc. Royal Soc., London Ser. A, **440** (1993) no. 1908, 201–220.

[8] P. Balister, B. Bollobás, R. Kozma, (2003) "Mean Field Models of Probabilistic Cellular Automata", *Random Structures and Algorithms,* Submitted

[9] P. Balister, B. Bollobás, R Johnson, M. Walters, (2003) "Random Majority Percolation", *Annals of Probability,* Submitted

[10] Barabási, A.L., "Linked: The New Science of Networks" (MA: Persus Publishing, 2002)

[11] Barabási, .L., E. Bonabeau "Scale-Free Networks", Scientific American 288, 60-69 (2003)

[12] Barrie JM. Freeman WJ, Lenhart M. Modulation by discriminative training of spatial patterns

of gamma EEG amplitude and phase in neocortex of rabbits. J. Neurophysiol. 1996, 76: 520-539.

[13] Berlekamp, E.R., JH Conway, and RK Guy, "Winning Ways for your mathematical plays," Volume 1: Games in General, Academic Press, New York, NY, 1982.

[14] Binder, K. "Finite scale scaling analysis of Ising model block distribution function," Z. Phys. B. 43, 119-140, 1981.

[15] B. Bollobás, (1985) "Random Graphs," Academic Press, London, Orlando

[16] Bollobás, B., Riordan, O., Results on scale-free random graphs. Handbook of graphs and networks, 1–34, Wiley-VCH, Weinheim, 2003.

[17] Bressler SL, Kelso JAS. Cortical coordination dynamics and cognition. Trends in Cognitive Sciences, 2001, 5:26-36.

[18] Bressler SL. Understanding cognition through large-scale cortical networks. Current Directions in Psychological Science, 2002, 11:58-61.

[19] Bressler SL. Cortical coordination dynamics and the disorganization syndrome in schizophrenia. Neuropsychopharmacology, 2003, 28:S35-S39.

[20] R. Cerf and E.N. Cirillo, *Finite size scaling in three-dimensional bootstrap percolation.* Ann. Probab., **27** (1999) no. 4 1837–1850.

[21] B.A. Cipra, (1987) "An Introduction to the Ising Model," *Amer. Math. Monthly* **94,** 937-959.

[22] Crutchfield, J.P., The calculi of emergence: Computation, dynamics, and induction. Physica D, 1994. 75: p. 11-54.

[23] Dafilis, M.P., D. T. J. Liley and P. J. Cadusch, Robust chaos in a model of the electro-encephalogram: Implications for brain dynamics." Chaos (2001) 11, 474-478.

[24] A.M.S. Duarte, *Simulation of a cellular automaton with an oriented bootstrap rule*, Physica A, **157** (1989) 1075–1079.

[25] Erdos, P. and Renyi A. (1960). On the evolution of random graphs. Publ. Math. Inst. Hung. Acad. Sci. 5: 17-61.

[26] W. J. Freeman (1975) *"Mass Action in the Nervous System,"* Academic Press New York, San Francisco, London

[27] W.J. Freeman, *Noise-induced first-order phase transitions in chaotic brain activity*, Int. J. Bifurcation & Chaos, **9** (1999) (11) 2215–2218.

[28] Freeman WJ, "The wave packet: An action potential for the 21st Century. ", J. Integrative

Neurosci., p. 3, vol. 2, (2003).

[29] Freeman, W.J., "Evidence from human scalp EEG of global chaotic itinerancy", Chaos, p. 1067, vol. 13, (2003).

[30] Freeman WJ, Burke BC, Holmes MD. (2003): Aperiodic phase re-setting in scalp EEG of beta-gamma oscillations by state transitions at alpha-theta rates. Human Brain Mapping 19:248-272.

[31] Freeman WJ, Burke BC, Holmes MD, Vanhatalo S. (2003): Spatial spectra of scalp EEG and EMG from awake humans. Clin Neurophysiol 16:1055-1060.

[32] Freeman WJ (2003) A neurobiological theory of meaning in perception. Part 1. Information and meaning in nonconvergent and nonlocal brain dynamics. Int. J. Bifurc. Chaos 13: 2493-2511.

[33] Friston KJ. (2000): The labile brain. I. Neuronal transients and nonlinear coupling. Phil Trans R Soc Lond B 355:215-236.

[34] Haken, H. What can synergetics contribute to the understanding of brain functioning? In: Analysis of Neurophysiological Brain Functioning. Uhl, C, (ed.) Berlin: Springer-Verlag. pp. 7-40, 1999.

[35] Freeman, W.J., Holmes, M.D., West, G.A., Vanhatalo, S. (2004) Dynamics of Human Neocortex that Optimize its Stability and Flexibility (submitted)

[36] Gacs, P. A Toom rule that increases the thickness of sets. J. Statist. Phys. 59 (1990), no. 1-2, 171–193.

[37] J. Gravener and E. McDonald, *Bootstrap percolation in a polluted environment*, J. of Statist. Phys., **87** (1997) nos. 3–4 915–927.

[38] G. Grimmett, *Percolation in Fundamental Principles of Mathematical Sciences*, Springer-Verlag, Berlin, (1999) *xiv*+444pp.

[39] Hopfield, J.J.,(1982). Neural networks and physical systems with emergent collective computational abilities, Proc. National Academy of Sciences, USA, 79, 2554-2558.

[40] Hoppensteadt, F.C. and Izhikevich E.M. Thalamo-cortical interactions modeled by weakly connected oscillators: could the brain use FM radio principles? BioSystems 1998, 48: 85-94.

[41] Ingber L. Statistical mechanics of multiple scales of neocortical interactions. pp. 628-681 in: Nunez PL (ed.). Neocortical Dynamics and Human EEG Rhythms. New York: Oxford U.P., 1995.

[42] Jensen, H.J. "Self-organized criticality - Emergent behavior in physical and biological systems," Cambridge University Press, 1998.

[43] Kaneko, K. (1990). Clustering, coding, switching, hierarchical ordering, and control in a network of chaotic elements, Physica D, 41, 137-172.

[44] Kaneko K, Tsuda I. Complex Systems: Chaos and Beyond. A Constructive Approach with Applications in Life Sciences, 2001.

[45] Kauffman, S.A., *Requirements for evolvability in complex systems: orderly dynamics and frozen components*, Physica D, **42** (1990) 135–152.

[46] Korn, H., P. Faure, Is there chaos in the brain? II. Experimental evidence and related models, Comptes Rendus Biologies 326 (2003) 787-840

[47] R. Kozma, *Intermediate-range coupling generates low-dimensional attractors deeply in the chaotic region of one-dimensional lattices*, Phys. Lett. A, **244** (1998) (1–3) 85–91.

[48] Kozma, R., Freeman, W.J., "Chaotic Resonance - Methods and Applications for Robust Classification of Noisy and Variable Patterns," International Journal Bifurcation and Chaos, 11, pp.1607-1629, 2001.

[49] R. Kozma, P. Balister, B. Bollobás, W.J. Freeman, (2001) "Dynamical Percolation Models of Phase Transitions in the Cortex," in: Proc. *NOLTA 01 Nonlinear Theory and Applications Symposium, Miyagi, Japan,* Vol. 1, pp. 55-59.

[50] R. Kozma, P. Balister, B. Bollobás, H. Chen, and W.J. Freeman, (2003) "Analysis of Scaling Laws in a Local Random Cellular Automata Model," *Submitted*

[51] Kozma, R., Puljic, M., Balister, P., Bollobás, B., Freeman, W.J. (2004) Neuropercolation: A Random Cellular Automata Approach to Spatio-Temporal Neurodynamics," Lect. Notes Comp. Sci., LNCS Vol. 3350, pp. 435-443, Springer Verlag.

[52] Linkenkaer-Hansen, K., Nikouline, V.M., Palva, J.M., Iimoniemi, R.J. Long-range temporal correlations and scaling behavior in human brain oscillations. J. Neurosci. 2001, 15: 1370-1377.

[53] Maes, C., Vande Velde, K. Relative energies for non-Gibbsian states. Comm. Math. Phys. 189 (1997), no. 2, 277–286.

[54] Makowiec, D. "Stationary states for Toom cellular automata in simulations,"(1999) Phys. Rev. E **55,** 3795

[55] Marcq, P., H. Chaté, and P. Manneville, *Universality in Ising-like phase transitions of lattices of coupled chaotic maps*, Phys. Review E, **55** (1997) no. 3 2606–2627.

[56] Ohl, F.W., Scheich, H. and Freeman, W.J. (2001) Change in pattern of ongoing cortical activity with auditory category learning. Nature 412: 733-736.

[57] Ohl, F.W., Deliano, M., Scheich, H., Freeman, W.J. (2003) Early and late patterns of stimulus-related activity in auditory cortex of trained animals. Biol. Cybernetics online: DOI 10.1007/s00422-002-0389-z

[58] A. Peters, S.L. Palay, and H. deF. Webster, (Fine Structure of the Nervous System: Neurons and Their Supporting Cells, Oxford University Press, New York and Oxford, 1991).

[59] Y. Pomeau, *Periodic behavior in cellular automata*, J. of Statistical Physics, **70** (1993) (5–6) 1379–1382.

[60] Puljic M, Kozma R, (2003) "Phase Transitions in a Probabilistic Cellular Neural Network Model Having Local and Remote Connections, International Joint Conference on Neural Networks" IJCNN'2003, Portland, OR, July 14-19, 2003.

[61] Schiff, S.J. et al. (1994). Controling chaos in the brain, Nature, 370, 615-620.

[62] Skarda, C.A. and Freeman W.J., (1987). How brains make chaos in order to make sense of the world, Behavioral and Brain Sci., 10, 161-195.

[63] Stam, C.J., Breakspear, M., van Cappellen van Walsum A-M., van Dijk, B.W. (2003): Nonlinear synchronization in EEG and whole-head recordings of healthy subjects. Hum Brain Mapp 19:63-78.

[64] D. Stauffer, A. Aharony, (1994) *"Introduction to Percolation Theory,"* Selwood Printing Ltd, West Sussex, GB

[65] Toom,A.L., N.B.Vasilyev, O.N.Stavskaya, L.G.Mityushin, G.L.Kurdyumov and S.A.Prigorov (1990) Discrete local Markov systems in Stochastic cellular systems:ergodicity, memory, morphogenesis; eds. R.L.Dobrushin, V.I.Kryukov and A.L.Toom, Manchester University Press

[66] Wang XF, Chen GR. Complex networks: small-world, scale-free and beyond. IEEE Trans. Circuits Syst. 2003, 31: 6-20.

[67] Watts DJ, Strogatz SH. Collective dynamics of "small-world" networks. Nature 1998, 393: 440-442.